ORIGINAL PAPER - EXPLORATION GEOLOGY

Geochemistry and organic petrology of the bituminite shales from the Kapurdi mine, Rajasthan of NW India: implications for waxy oil generation potential

Mohammed Hail Hakimi[1] · Alok Kumar[2] · Alok K. Singh[3] · Aref Lashin[4] · Afikah Rahim[5] · Mikhail A. Varfolomeev[1] · Nura Abdulmumini Yelwa[6,7] · Khairul Azlan Mustapha[7]

Abstract

This study examines the geochemical and petrographic characteristics of seven bituminite shales from the Kapurdi mine in the Rajasthan, NW India, in order to assess their organic matter inputs and evaluate the oil-prone potentials. These bituminite shale samples exhibit high total organic carbon (TOC) content (up to 45.11 wt.%). The high TOC contents were correlated with low total sulfur content of less than 1 wt.% and suggest that these bituminite shales were deposited in a fresh lacustrine environment. The dominance of such lacustrine environmental setting was confirmed by the presence of the *Botryococcus* algae. The analyzed bituminite shales are characterized by a bimodal distribution of normal alkanes and relatively low isoprenoid Pr/Ph, Pr/n-C$_{17}$ and Ph/n-C$_{18}$ ratios. These characteristics suggest that these bituminite shales contain a blend of organic matter that was derived primarily from algal lacustrine and other aquatic organic matter, with terrigenous land plants and deposited under suboxic to anoxic environmental conditions. Such findings of the organic matter (OM) input and environmental conditions are consistent with mainly Types I and II kerogen and small amounts of Type II/III kerogen, thus yielding both oil and gas prone to higher concentrations of oil generation potential. The dominance of hydrogen-rich kerogen and oil generation potential is in agreement with the findings of high hydrogen index (HI = 240–425 mg HC/g TOC) and H/C atomic ratio of more than 1.20. The abundance of n-alkene and n-alkane doublets in the pyrolysis–gas chromatography (Py–GC) also indicates that these bituminite shales have potential to generate high concentrations of paraffinic waxy oil. Most of the maturity indicators show that the bituminite shales from the Kapurdi mine have not yet entered the main stage of oil generation window, exhibiting a range of immature stages. Therefore, as highlighted in this study, these bituminite shales can be considered as a good candidate for oil shale reoterting processes to release commercial amounts of oil upon using artificial heating techniques such as hydrothermal conversion.

Keywords Bituminite shale · Oil-generation potential · Hydrogen-rich liptinite maceral · Rajasthan · NW India

✉ Mohammed Hail Hakimi
ibnalhakimi@taiz.edu.ye

1 Department of Petroleum Engineering, Kazan Federal University, Kazan 420008, Russia

2 Department of Geology, Faculty of Science, University of Malaya, 50603 Kuala Lumpur, Malaysia

3 Department of Petroleum Engineering & Geo-Engineering, Rajiv Gandhi Institute of Petroleum Technology, Jais, Amethi 229304, India

4 College of Engineering-Petroleum and Natural Gas Engineering Department, King Saud University, Riyadh 11421, Saudi Arabia

5 Faculty of Engineering, School of Civil Engineering, Universiti Teknologi Malaysia, 81310 Johor Bahru, Johor, Malaysia

6 Department of Geology, Usmanu Danfodiyo University, P.M.B. 2346, Sokoto, Nigeria

7 Department of Geology, Faculty of Science, University of Malaya, 50603 Kuala Lumpur, Malaysia

Introduction

The Kapurdi mine is located in the northern Barmer Basin, along 25° 56′ 44″ N latitude and 71°21′ 17″ E longitude (Fig. 1). The Barmer Basin is associated with the intracratonic tectonic during the early Archean to Holocene period (Bhowmick 2008; Mathews et al. 2020). The Barmer Basin includes sedimentary successions, ranging in age between Mesozoic and Recent (Fig. 2) along with three significant unconformities (Mukherjee et al. 1992). The basin is also filled with thick organic-rich succession, including lignite and organic-rich shales (Fig. 3), with major distributions in the Cenozoic successions (Rana et al. 2005; Aggarwal et al. 2011; Raju and Mathur 2013; Paul and Dutta 2016; Shivanna and Singh 2016; Singh et al. 2020). The lignite deposits of the Eocene succession have received unprecedented attention from numerous researchers (Ambwani

Fig. 1 Right: Location map of the main basin in the Rajasthan, northwestern India, showing the Kapurdi mine location in the Barmer Basin and Left: Photomicrographs of the outcrop section in the Kapurdi mine
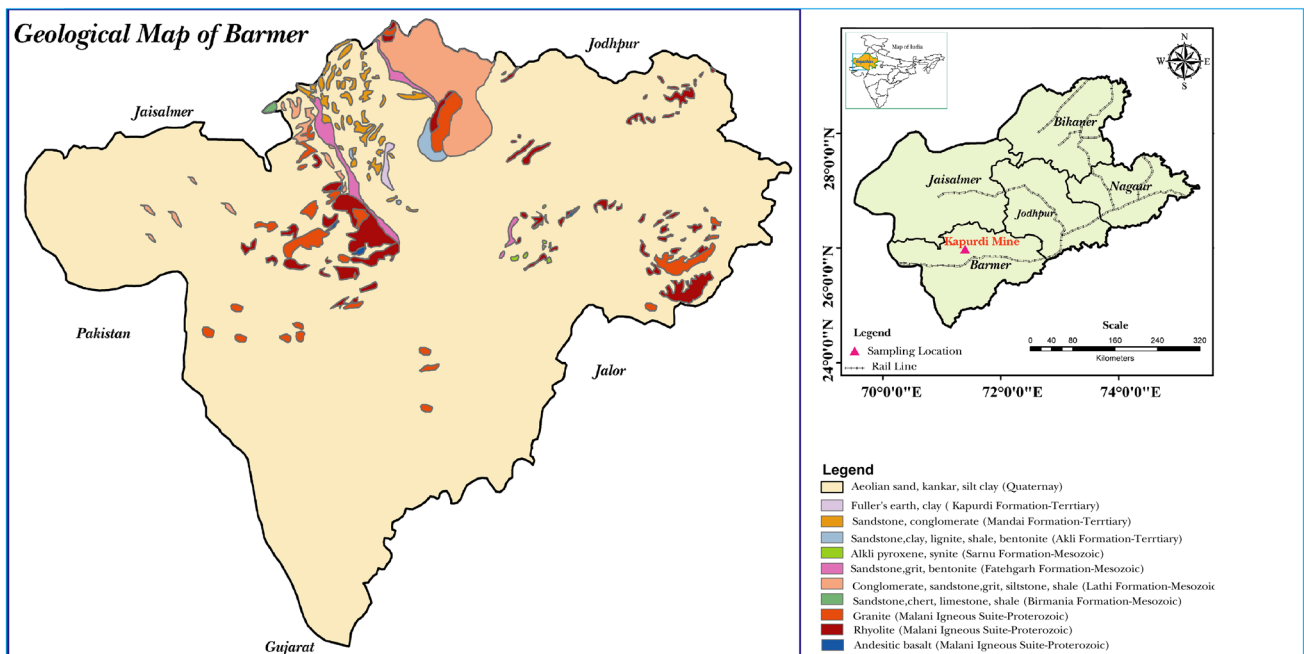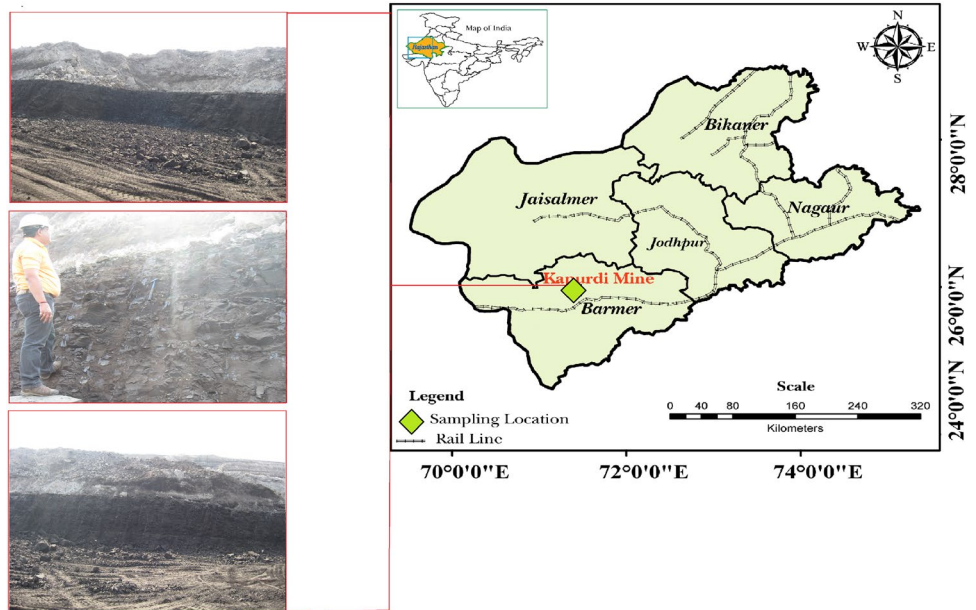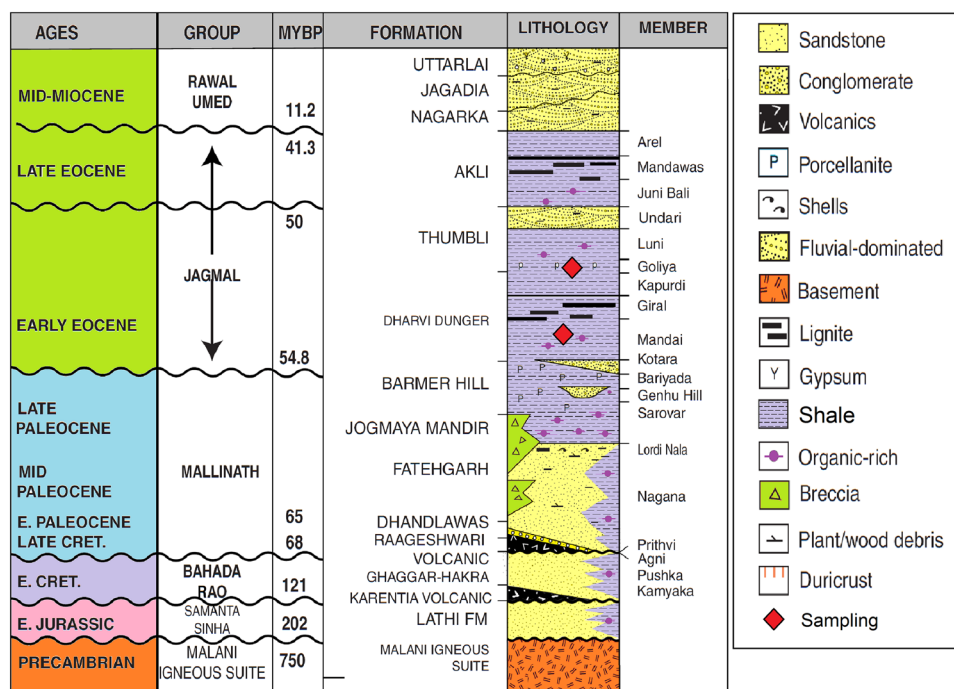

Fig. 2 Geological map of the Barmer Basin, including igneous rocks and sedimentary rocks

Fig. 3 Generalized stratigraphic succession in Barmer Basin, including organic-rich sedimentary sequence, ranging in age from Lower Jurassic to Eocene [modified after Dolson et al. (2015)]

and Singh 1996; Kar and Sharma 2001; Shukla et al. 2014; Singh et al., 2017; Singh and Kumar 2018; Mathews et al. 2020). As a result, the genesis, paleodepositional, climatic conditions and the petroleum generation potential of these lignite deposits were investigated based on organic and inorganic geochemistry analyses together with microscopic observations. However, limited works focused on the other organic-rich sediments of bituminite and carbonaceous shales in the Cenozoic successions. In this regard, the current study is focusing on the bituminite shale deposits within the Cenozoic succession from the Kapurdi mine, northern Barmer Basin, south western Rajasthan (Fig. 1).

In the Kapurdi mine, the Cenozoic succession consists of siltstone, sandstone, conglomerate, fullers' earth, bentonite, bituminite shale, and lignite (Mukherjee et al. 1992; Shivanna et al. 2017). The entire bituminite shales were obtained from the parting present within the lignite deposits of the Early Eocene succession (Fig. 3). These black shales (bituminite shale) were studied as an attempt to expand our knowledge on highlighting the characteristics of organic matter and evaluate its potential for conventional and unconventional resources for further petroleum exploration.

The objective of this study was to investigate the organic matter characteristics, including organic matter content, quality of organic matter (quantitatively and qualitatively), assess the thermal maturity level, and evaluate the petroleum generation potential by applying multiply geochemical techniques coupled with microscopic examinations. In addition, the *n*-alkane and isoprenoid distributions in the aliphatic hydrocarbon fraction of the extracted shale rocks together

with other geochemical and petrological results were discussed and used to assess the nature of organic matter input and environmental conditions at the time of deposition.

Geological background

Barmer Basin is an active rift basin, with a 200 km long and 40 km wide (Farrimond et al. 2015). It was formed as a result of the rapid separation of India plate from Africa plate during the Late Jurassic to Cretaceous (Dolson et al. 2015).

The lithostratigraphic column of the Barmer Basin is presented in Fig. 3. This basin contains clastic sediments ranging from the Mesozoic (Early Jurassic-Late Cretaceous) to Cenozoic (Early Paleocene to Mid Miocene), with the Cenozoic sedimentary succession having the greatest thickness (Fig. 3).

The Mesozoic sequence comprises Jurassic and Cretaceous formations, i.e., Lathi and Ghagga–Hakra (Fig. 3). The Early Jurassic Lathi sediments are mainly sandstones and subordinate shales and were deposited unconformably above the basement rocks of the Precambrian age (Fig. 3). The sandstone of the Lathi Formation is considered good quality reservoir in the Barmer Basin (Dolson et al. 2015).

The Lower Cretaceous Ghagga-Hakra Formation lies unconformably on the Lathi sediments comprising mainly non-marine (fluvial and lacustrine) sandstones (Fig. 3). The Ghagga-Hakra Formation also exhibits organic-rich shales and is considered as a potential source rock in the Barmer Basin (Dolson et al. 2015). The Ghagga–Hakra

Formation overlies by the Deccan Trap volcanics (Upper Cretaceous–Lower Paleocene). The Deccan volcanics make a conformable contact with the Mesozoic (Late Cretaceous) and Cenozoic (Early Paleocene) sequences. The Cenozoic (Early Paleocene-Mid Miocene) sequence in the basin comprises many formations, namely Fatehgarh, Barmer Hill, Dharvi/Dungar, Thumbli, Akli Nagarka, Jagadia, and Uttarlai (Fig. 3).

The Fatehgarh Formation is dominated by organic-rich shale and sandstone intervals accumulated in braided to meandering channels (Dolson et al. 2015). These sandstone intervals are regarded as important reservoir rocks in the Barmer Basin, with porosity and permeability values ranging from 17 to 33% and 200 to 20,000 mD, respectively (Dolson et al. 2015). During the Late Paleocene, mainly lacustrine shale and sandstone sediments of the Barmer Hill Formation were deposited conformably above the Fatehgarh

Formation (Fig. 3). The Barmer Hill Formation is followed by the Early Eocene Dharvi/Dungar and Thumbli formations, which consists of black shale intercalated with lignite (Fig. 4). The black shale unit of the Early Eocene Dharvi/Dungar and Thumbli formations was deposited in lacustrine environmental setting (Dolson et al. 2015). The Late Eocene Akli Formation follows the early Eocene Dharvi/Dungar and Thumbli formations, with unconformable contact (Fig. 3). It contains of lacustrine black shale intervals with interbedded swamp lignites (Dolson et al. 2015). It is followed by the Mid Miocene formations (Nagarka, Jagadia, and Uttarlai) (Fig. 3). This young geologic sequence lies unconformably on the Akli sediments (Fig. 3) and mainly composed of cross-bedded sandstone intervals (Dolson et al. 2015).

Fig. 4 Photomicrographs of organic matter assemblages from the analyzed bituminite shale rocks; under UV light, field width = 0.2 mm, including structured and unstructured fluorescence liptinite of sporinite, cutinite, alginite, resinite and bituminite, respectively
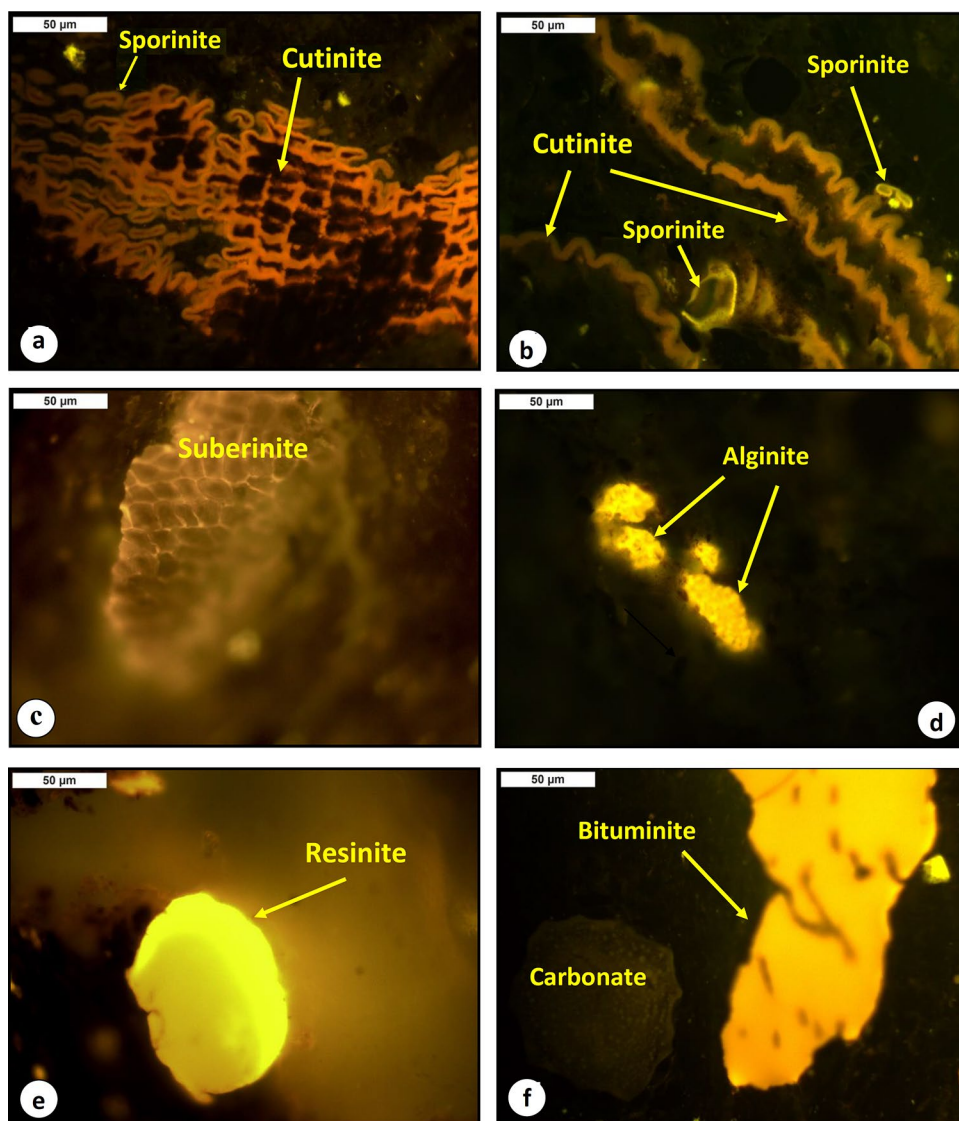
Table 1 Geochemical and organic petrographic results of the analyzed bituminite shale samples from Kapurdi mine in the Barmer Basin, NW India; including TOC, TS contents, bulk Rock–Eval pyrolysis, pyrolysis–gas chromatography (Py–GC), normal alkanes and isoprenoids, atomic ratios, huminite/vitrinite reflectance (VR_o %) and maceral counting percentage along with basis of mineral matter (vol.%) and mineral-matter-free (vol.%)

Organic petrographic results

Sample id	Maceral composition (%)			Mineral matter (%)	Maceral composition (free minerals %)			Huminite/vitrinite reflectance (VR_o %)			
	Huminite	Liptinite	Inertinite		Huminite	Liptinite	Inertinite	Mean	Minimum	Maximum	SD
KD-M1	8.14	14.51	0.00	77.35	35.94	64.06	0.00	0.30	0.21	0.36	0.042
KD-M2	6.87	11.21	0.36	81.56	37.26	60.79	1.95	0.35	0.22	0.49	0.067
KD-M3	9.36	17.88	0.62	72.14	33.60	64.18	2.23	0.26	0.23	0.40	0.053
KD-M4	12.62	4.48	0.80	82.10	70.50	25.03	4.47	0.32	0.27	0.44	0.042
KD-M5	26.87	11.33	0.42	61.38	69.58	29.34	1.09	0.33	0.22	0.41	0.051
KD-M6	24.02	10.54	3.78	61.66	62.65	27.49	9.86	0.33	0.21	0.42	0.043
KD-M7	8.71	6.57	1.54	83.18	51.78	39.06	9.16	0.35	0.22	0.44	0.047

Organic geochemical results

Sample id	TOC (wt.%)	TS (wt.%)	Rock–Eval pyrolysis									Atomic ratios		Pyrolysis–gas chromatography (Py–GC)					
			S_1	S_2	S_3	T_{max}	HI	OI	PY	PI	S_2/S_3	H/C	O/C	n-C_9 (%)	Xylene (%)	2-,3-dimethylthiophene (%)	C_1-C_5 (%)	C_6-C_{14} (%)	+C_{15} (%)
KD-M1	21.39	0.47	1.57	73.93	8.40	423	346	39	75.50	0.02	8.80	1.59	0.45	57.95	29.49	12.56	28.50	31.30	40.20
KD-M2	22.81	0.49	2.2	78.53	9.08	422	344	40	80.73	0.03	8.65	1.53	0.42	54.52	32.16	13.32	22.61	35.34	42.05
KD-M3	43.03	0.61	7.59	182.69	14.61	420	425	34	190.28	0.04	12.50	1.27	0.76	59.63	24.46	15.90	27.57	29.72	42.71
KD-M4	9.44	0.35	0.38	22.74	1.76	426	240	18	23.12	0.02	12.92	1.21	0.43	41.07	30.07	19.87	21.16	30.39	48.45
KD-M5	33.34	0.34	2.97	117.82	5.92	424	353	17	120.79	0.03	19.90	1.37	0.46	43.28	37.80	18.92	22.50	33.30	42.30
KD-M6	45.11	0.91	5.83	174.04	6.52	425	385	14	179.87	0.03	26.69	1.28	0.71	38.88	33.83	27.29	20.61	37.34	40.05
KD-M7	16.73	–	0.75	46.46	3.51	429	277	20	47.21	0.02	13.24	1.53	0.44	47.32	32.54	20.13	24.77	32.52	41.71

Normal alkanes and isoprenoids

Sample id	Pr/Ph	Pr/n-C_{17}	Ph/n-C_{18}	CPI
KD-M1	2.60	0.69	0.30	2.30
KD-M2	2.70	0.54	0.20	2.15
KD-M3	1.17	0.20	0.31	1.98

2,3 Dimeth. (%)—percent concentration of 2,3 dimethylthiopene in relation to O-xylene and n-C9, O-xylene (%)—percent concentration of O-xylene in relation to 2,3 dimethylthiopene and n-C9, n-C9 (%)—percent concentration of n-C9 in relation to 2,3 dimethylthiopene and O-xylene

Pr Pristane; *Ph* Phytane; *CPI* Carbon Preference Index (1): $\{2(C_{23}+C_{25}+C_{27}+C_{29}) / (C_{22}+2[C_{24}+C_{26}+C_{28}]+C_{30})\}$

TOC total organic carbon, wt. %, *TS* total sulfur, wt.%, S_1: Volatile hydrocarbon (HC) content, mg HC/ g rock, S_2: Remaining HC generative potential, mg HC/g rock, S_3: carbon dioxide content, mg CO_2/g rock, T_{max} temperature at maximum of S_2 peak, *HI* Hydrogen Index = $S_2 \times 100$/TOC, mg HC/g TOC, *OI* Oxygen Index = $S_3 \times 100$/TOC, mg CO2/g TOC, *PY* Potential Yield = $S_1 + S_2$ (mg/g), *PI* Production Index = $S_1/(S_1 + S_2)$

Dataset and methods

A total number of seven outcrop samples were taken from the Kapurdi mine site (Fig. 1). These outcrop samples exhibit the bituminite shales that were mainly collected from the lignite rock unit (Fig. 1). The samples were cleaned before geochemical and petrological analyses to eliminate impurities such as weathering and oxidation.

The bituminite shale samples were subjected to multi-geochemical analyses, utilizing total organic carbon (TOC) and sulfur (TS) contents, Rock–Eval programmed pyrolysis analysis, ultimate analysis, pyrolysis–gas

chromatography (Py–GC), bitumen extraction and gas chromatography–mass spectrometry (GC–MS), along with microscopic examinations of the maceral types and reflectance measurements of huminite/vitrinite (VR_o %).

Total organic carbon content (TOC), programmed pyrolysis (Rock–Eval-6) analysis

The seven shale samples were ground to generate standardized powder for the source rock geochemical analyses such as TOC content and programmed pyrolysis.

A 100 mg powdered (< 200 mesh size) was utilized to evaluate TOC content using a LECO CS244 Carbon/Sulfur Analyzer instrument, and the results were primarily expressed as weight percentages (TOC wt.%).

The seven shale samples also underwent programmed pyrolysis with a programmed oven temperature between 300 and 600 °C. Rock–Eval 6 instrument was used to measure the bulk pyrolysis on the powdered samples according to the procedure outlined by Espitalie et al. (1977) and Lafargue et al. (1998).

This instrument was used to evaluate the petroleum yields such as free petroleum (S1, mg HC/g rock) and hydrocarbon yield from kerogen cracking (S2, mg HC/g rock) at a temperature between 300 and 600 °C. The S_3 peak also released during programmed pyrolysis, which represents the quantity of CO_2 formed by pyrolysis of the organic matter and expressed in milligrams of CO_2 per gram of rock (mg/g).

The maximum temperature (T_{max}) of S_2 peak was also measured during pyrolysis analysis (Table 1). Because T_{max} refers to the temperature at which the maximum S_2 peak yield is most reliable when the S_2 values surpass 1 mg/g rock, it is employed for samples with S_2 values above 1 mg HC/g TOC (Jarvie et al. 2001; Katz and Lin 2021).

Furthermore, the geochemical parameters like hydrogen index (HI), oxygen index (OI) and production index (PI) were also determined (Shown in Table 1), following the studies of Peters and Cassa (1994).

Ultimate elemental analysis

The ultimate analysis was also performed on the bituminite shale samples following the standards of ASTM D3176-09 (2009). The whole fine grounded samples were analyzed
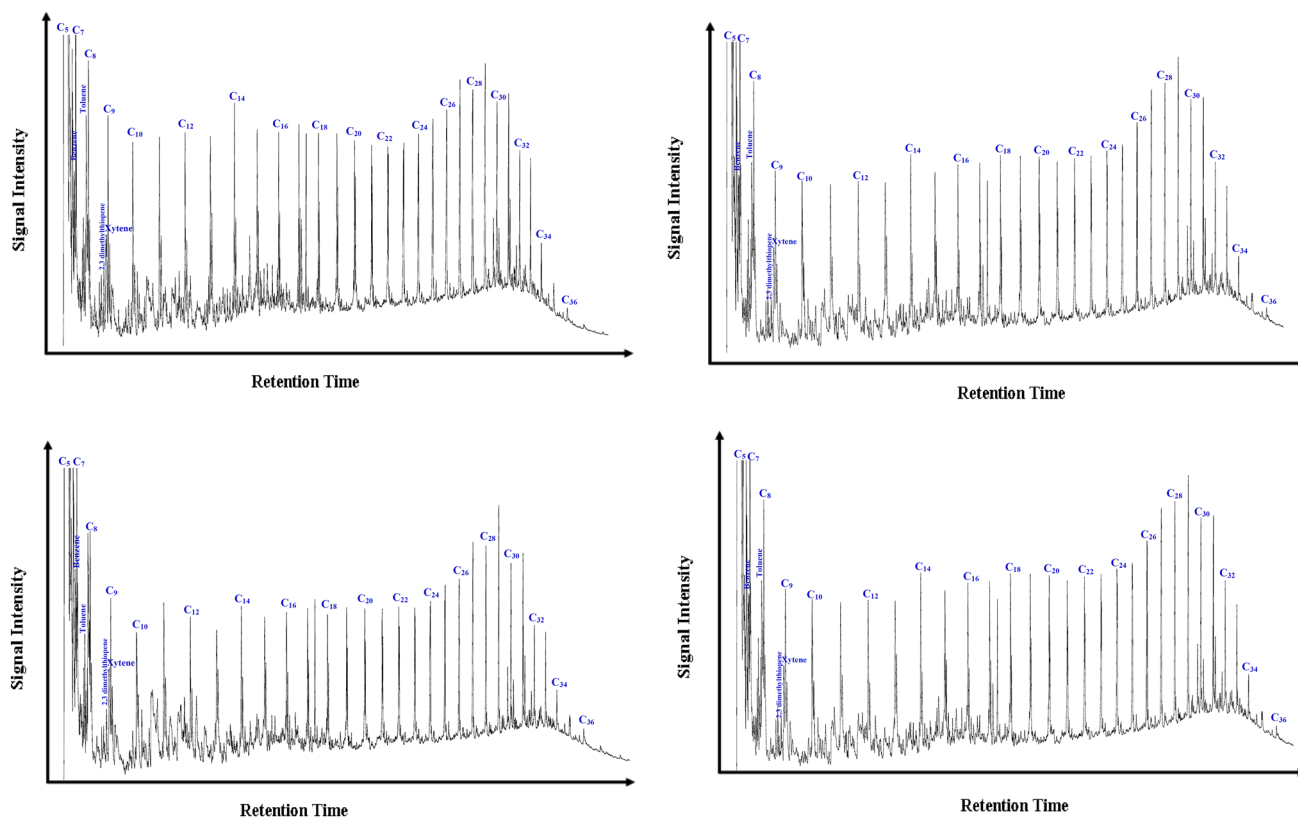
Fig. 5 Pyrolysis GC pyrograms of the four analyzed bituminite shale samples, showing labeled peaks of *n*-alkene and *n*-alkane doublets, sulfur-lean organic matter, and aromatic hydrocarbons (toluene, xylene, and benzene) used as kerogen and petroleum-type proxies (see Figs. 11A and 13B)

using an elemental analyzer to measure carbon, hydrogen, nitrogen and sulfur (CHNS) contents in percentage. Subsequently, the oxygen content was calculated based on the difference in the percentages of the CHNS contents. The atomic ratios of H/C and O/C were then calculated following the procedure of ASTM D3176-09 (2009).

Open pyrolysis–gas chromatography (Py–GC)

The seven shale samples were subsequently subjected to open pyrolysis–gas chromatography (Py–GC) and used to obtain information on kerogen characteristics and compositions (Dembicki et al. 1983; Horsfield 1989; Dembicki 1993; Abbassi et al. 2016).

The Py–GC examines ~2 mg of each sample, applying a Frontier Lab Pyrolyzer System in thermal desorption (40–330 °C) and pyrolysis (600 °C) as outlined by Larter

Fig. 6 Normal alkane and isoprenoid distribution according to m/z 85 of the three studied bituminite shale samples

(1984). The Py–GC analysis was programmed from 40 to 300 °C before pyrolyzate flowed through the GC column between 300 and 600 °C. The chromatography of the pyrolyzates at 600 °C shows a methane spike followed by a set of *n*-alkane and *n*-alkene double spikes, along with a few aromatic peaks occurring among them.

Bitumen extraction and gas chromatography–mass spectrometry (GC–MS)

Representative three shale samples were subjected to the extraction process and gas chromatography–mass spectrometry (GC–MS) analysis.

The soluble bitumen was extracted using an azeotropic mixture of dichloromethane (DCM) with methanol (CH_3OH) with a ratio of 93:7 for approximately 72 h. The extracted bitumen in these shale rocks was fractionated into three fractions aliphatic and aromatic hydrocarbons and polar (NSO) compounds using liquid column chromatography with silica gel.

In addition, the aliphatic fraction was analyzed by applying Agilent 5975B inert MSD gas chromatography-mass spectrometry (GC–MS) using a HP-5MS column, with temperature ranging from 40 to 340 °C at a rate of 4 °C/min and a holding time of 30 min at 300 °C. The GC–MS analysis was employed to assess the lipid biomarkers in the saturate hydrocarbon fraction such as *n*-alkanes and isoprenoids applying specific ions, e.g., m/z 85, and their proportions and parameters were measured from their peak heights.

Organic petrology

The seven shale bituminite samples also underwent microscopic examinations comprising maceral types and reflectance measurements of huminite/vitrinite (VRo) under plane-polarized reflected white and ultraviolet (UV) lights.

The polished sample blocks were investigated under microscope for the identification of organic facies. In this case, entire whole shale samples were broken into pea-sized fragments (~2–3 mm) and placed in molds through a mixture of Serifix resin and cold-mount hardener. Being hardened, the blocks were grounded to expose the sample surfaces using silicon carbide papers with varying grit sizes; then, they were singly polished using alumina powder and oxide-polishing suspension solution.

The polished blocks then underwent examination using oil immersion under both reflected white and ultraviolet (UV) light using a LEICA DM 2700P optical microscope coupled with fluorescence illuminators photometry microscope. The quantitative and qualitative analyses of maceral types, including huminite, liptinite, and inertinite, were carried out following ICCP (2001), Sýkorová et al. (2005),
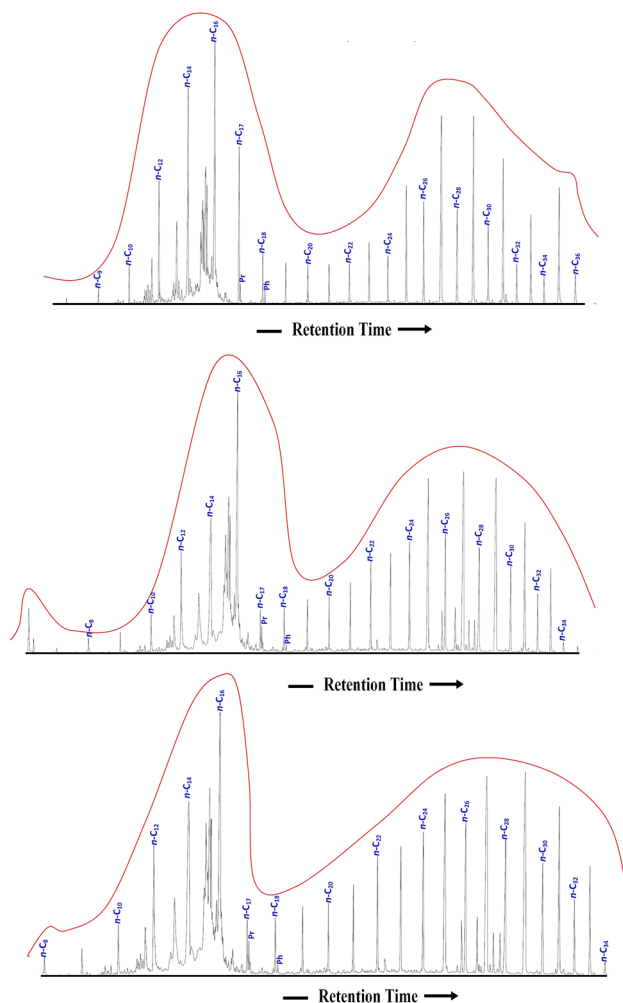
Fig. 8 Cross-plot of the sulfur and TOC contents (wt.%), suggesting a lacustrine environment during deposition of the analyzed bituminite shales
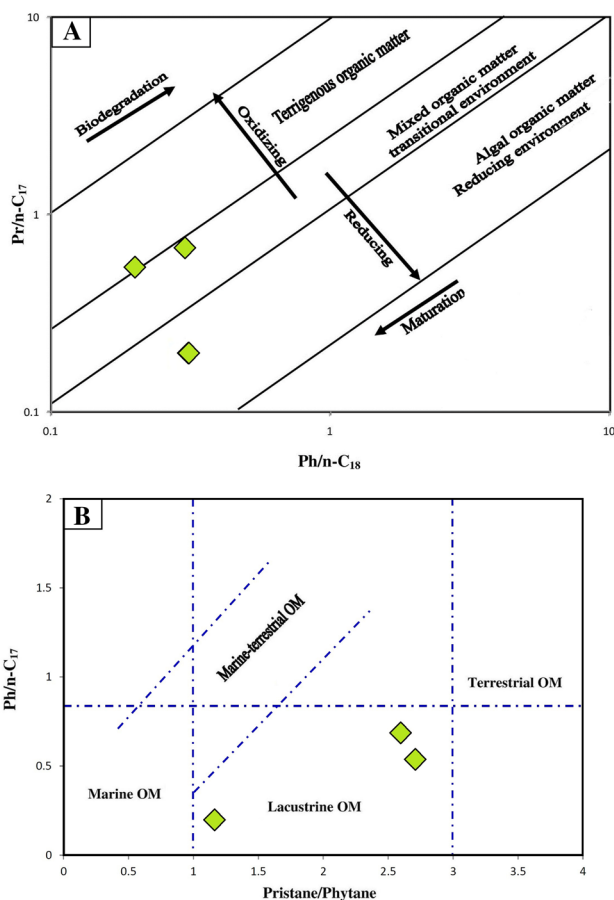
Fig. 7 Biomarker cross-plots of isoprenoid ratios: Pr/Ph, Pr/C17, and Ph/C18, show that the analyzed bituminite shale samples received a high contribution of algal organic matter and deposited in a lacustrine environment under reducing conditions, ranging from suboxic to anoxic

Hower and Wagner (2012), and Pickel et al. (2017). In this case, reflected UV lights were used to discriminate maceral types for each sample.

In addition, the reflectance of huminite/vitrinite (VR$_o$) measurements was also performed on the polished blocks using reflected white light. The huminite/vitrinite (VR$_o$ %) reflectance was measured after calibration using a reflectance standard value of 0.42% under oil immersion, in a white plane-polarized reflected light using a DM 2700P Leica Microsystems, and the mean of reflectance values was calculated for 25 measurements per sample.

Results and interpretation

Organofacies characterization (organic petrology)

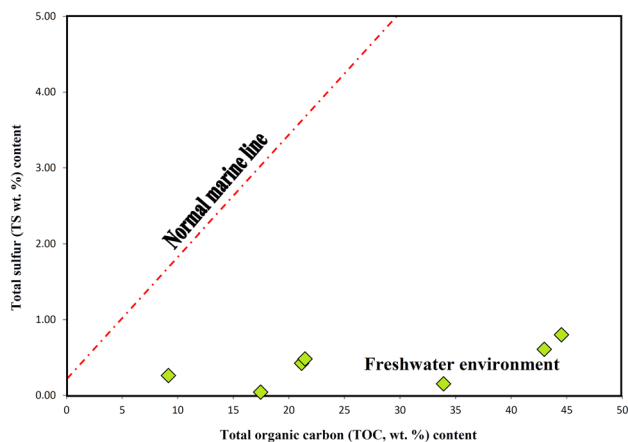Microscopic examinations were carried out to identify maceral types in the analyzed bituminite shales. The overall composition of the macerals was determined on the basis of mineral matter and mineral matter free with the observations is presented in Table 1. The results show that these bituminite shale samples are entirely dominated by mineral matter between 61.38 and 83.18% (Table 1). The shale samples have a high abundance of the huminite and liptinitic macerals that were derived from terrestrial organic matter, ranging from 33.60 to 70.50% and 25.03 to 64.18%, respectively (Table 1). The occurrence of inertinite macerals of the terrestrial organic matter is also commonly present in the studied samples in the range of 1.09–9.86% (Table 1).

The results of the optical observations under the UV-light excitation show that most of the hydrogen-rich liptinite macerals are structured and unstructured organic matter and are characterized by fluorescence intensities ranging from orange to yellow (Fig. 4). Most of the structured organic matter includes suberinite, sporinite, cutinite and alginite (Fig. 4). Sporinite occurs as a ring-agglomerated form and is commonly associated with cutinite maceral. Both sporinite and cutinite macerals are characterized by yellow to orange-yellow fluorescence (Fig. 4a and b). Suberinite maceral is also represented and characterized by cell-wall tissue and has fluorescence intensities ranging from brownish-yellow to yellow (Fig. 4c). Hydrogen-rich liptinite, i.e., alginate, is also obtained in some samples, which was primarily presented as *Botryococcus* (Fig. 4d).

In addition, resinite and bituminite are also found as unstructured liptinite macerals in the studied bituminite shale samples (Fig. 4e and f). Resinite mainly takes the form of isolated globular bodies with various shapes and is characterized by high fluorescence intensities ranging from greenish-yellow orange to bright yellow (Fig. 4e). A small portion of bituminite was also found with an irregular

Fig. 9 Geochemical correlations between TOC content and PY ($S_1 + S_2$) parameter, implying that the analyzed bituminite shales from Kapurdi mine location in the northern Barmer Basin are considered to be very good to excellent source rock and can generate significant amounts of petroleum during the thermal maturation
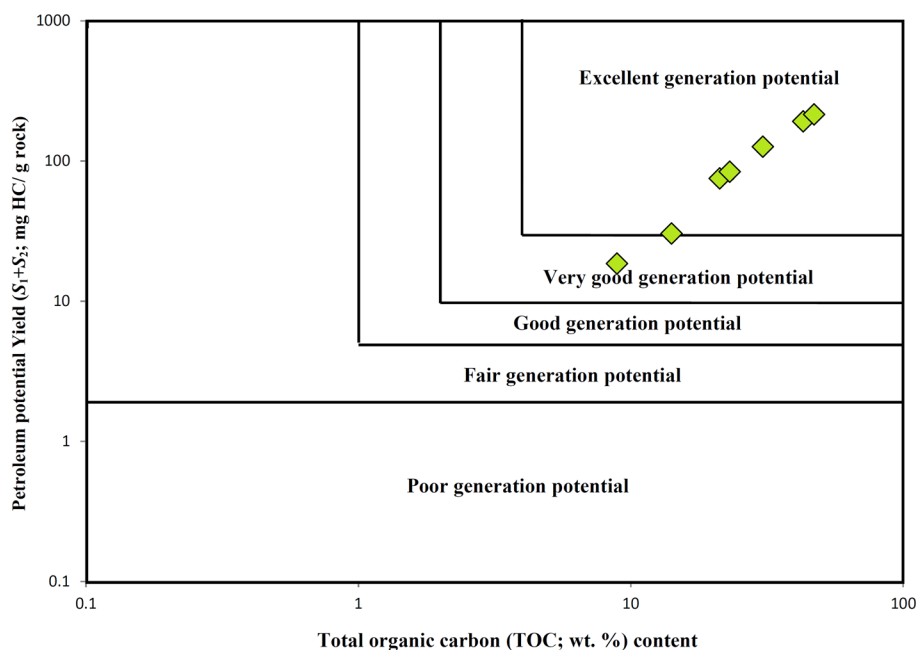
surface and characterized by an orange to brownish-yellow fluorescence (Fig. 4f).

Total organic carbon (TOC) and total sulfur (TS) contents

The organic carbon content (TOC) is commonly inferring the presence of organic matter richness (Bissada 1982; Jarvie 1991; Peters 1986; Peters and Cassa 1994; Katz and Lin 2014).

In this study, the TOC content measurements are conducted for all the bituminite shale samples and as expected the studied samples have high TOC content between 9.44 and 45.11 wt.% (Table 1). Majority of the measurements indicate high TOC > 20 wt.% (21.39–45.11%); meanwhile, two samples exhibit less TOC content between 9.4 and 16.73% (Table 1). The TOC contents of the studied shale samples, overall, indicate organic matter richness.

The total sulfur (S) content in the studied bituminite shale samples was found to be in its lowest amounts, between 0.34 and 0.91 wt.% (Table 1). However, the S content is usually employed to investigate the depositional environments of marine versus non-marine (e.g., Berner and Raiswell 1983). A high S content of more than 1 wt.% implies a marine environment (Hakimi et al. 2016), while a low S content of less than 0.5 wt.% suggests a non-marine environment (freshwater) (Berner and Raiswell 1983; Makeen et al. 2015). Accordingly, the low S content of < 1 wt.% demonstrates that the analyzed samples were deposited in a freshwater environmental setting (i.e., lacustrine).

Programmed pyrolysis (RE) and ultimate elemental

Table 1 also summarizes the S_1, S_2, S_3, HI, OI and PI values obtained by Rock–Eval pyrolysis of the seven bituminite shale samples. The results show that the petroleum generated by the thermal cracking of kerogen (S_2) yield is high and found to be the range of 22.74–182.69 mg HC/g rock. Most of the samples ($n = 5$) have S_2 values greater than 70 mg hydrocarbon/g rock (range 73.93–182.69 mg hydrocarbon/g rock), while two samples have S_2 yields ranging from 22.74 to 46.46 mg hydrocarbon/g rock (Table 1). The pyrolysis data, on other hand, revealed that the free petroleum (S_1) yield in most of the examined samples ($n = 5$) is substantial, ranging from 1.57 to 7.59 mg hydrocarbon/g rock (Table 1). Two samples show the lowest values of S1 of less than 1 mg hydrocarbon/g rock (Table 1).

In addition, the T_{max}, values based on the S_2 generation of the analyzed shale samples were found to be more than 1 (22.74–182.69 mg HC/g rock) as shown in Table 1. Therefore, the most reliable Rock–Eval T_{max} data were attained between values of 420–429 °C (Table 1).

The HI and OI parameters were calculated utilizing the compatibility of pyrolysis S_2 and S_3 yields with TOC content, respectively (Table 1). The HI values of the analyzed samples are substantial, ranging from 240 to 425 mg hydrocarbon/g TOC (Table 1). Most of the analyzed samples ($n = 5$) have HI values of more than 300 mg HC/g TOC, with values ranging from 344 to 425 mg HC/g TOC (Table 1). However, two samples show the lowest HI values between 240 and 277 mg HC/g TOC (Table 1). In terms of OI values, most of the samples have values of ᐸ50 mg CO_2/g TOC (14–40 mg CO_2/g TOC; Table 1).

Fig. 10 Geochemical correlations between Rock–Eval hydrogen index (HI), oxygen index (OI), and T_{max}, and H/C vs. O/C atomic ratios, showing that the analyzed bituminite shale samples are dominated by oil-prone kerogen types (Type I and II), with small amounts of mixed II/III kerogen
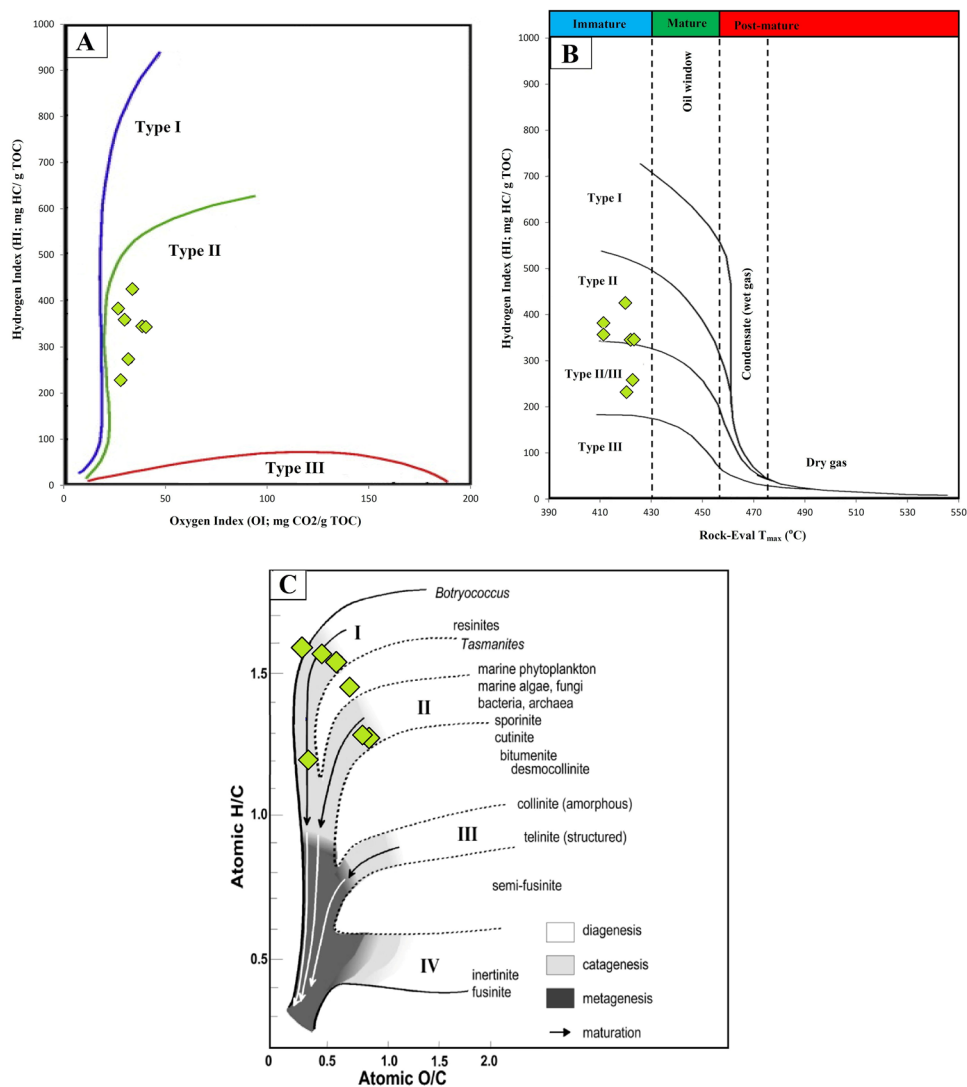
The H/C and O/C atomic ratios were also obtained in addition to the HI and OI data (Table 1). The H/C atomic values are substantial and found to be in the range between 1.21 and 1.58 (Table 1). In contrast, the analyzed samples have low O/C atomic values of less than 1, ranging from 0.42 to 0.76 (Table 1).

Open pyrolysis–gas chromatography (Py–GC)

The Py–GC method which employs the distributions of *n*-alkene and *n*-alkane doublets coupled within light aromatic hydrocarbon of the pyrolyzate S_2 provides a critical insight about the kerogen composition and petroleum-generating facies in the investigated samples (Dembicki 1993, 2009; Horsfield 1989; Dembicki et al. 1983; Abbassi et al. 2016). In this study, the Py–GCs of pyrolyzate S_2 in the representative four samples are shown in Fig. 5. The

chromatograms show bimodal distributions of the carbon peaks, ranging from C_5 to beyond C_{30} of *n*-alkene and *n*-alkane aliphatic compounds. The *n*-alkane and *n*-alkene compounds in most of the samples are highly concentrated in low and high molecular carbon fractions. The aromatic hydrocarbons are also present in low concentrations and are mainly toluene, xylene, and benzene alkylbenzenes. Besides aliphatic and aromatic hydrocarbons, the pyrolyzates also include low amounts of 2, 3-dimethylthiophene (Fig. 5).

Normal alkane and isoprenoid distributions

In the current study, the hydrocarbon distributions of *n*-alkane along with acyclic isoprenoids (i.e., pristane and phytane) in the saturated HC fraction of the representative three extracted shale rocks were examined and are shown in chromatograms of GC (Fig. 6), and their ratios and parameters are presented in Table 1. In the chromatograms of
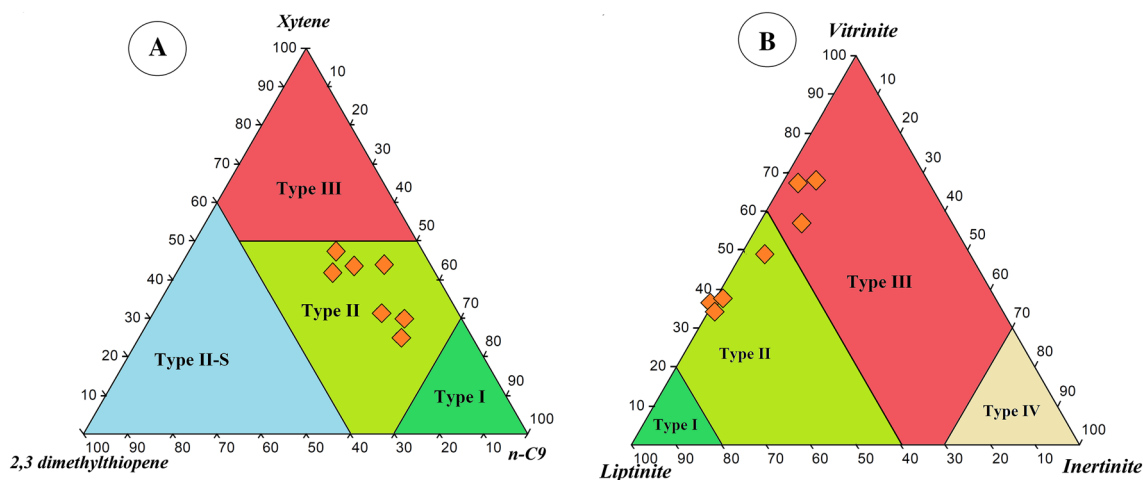
Fig. 11 Ternary diagrams on the kerogen characteristics based on (**A**) the relative percentage of compounds 2, 3-dimethylthiophene, O-xylene (1, 2- dimethylbenzene) and n-non-1-ene (n-C9:1) derived from the n-alkyl chain length distribution in the Py-GC data (see Fig. 5) and (**B**) the relative percentage of maceral types, showing that the analyzed bituminite shale samples are dominated by oil-prone Type II kerogen
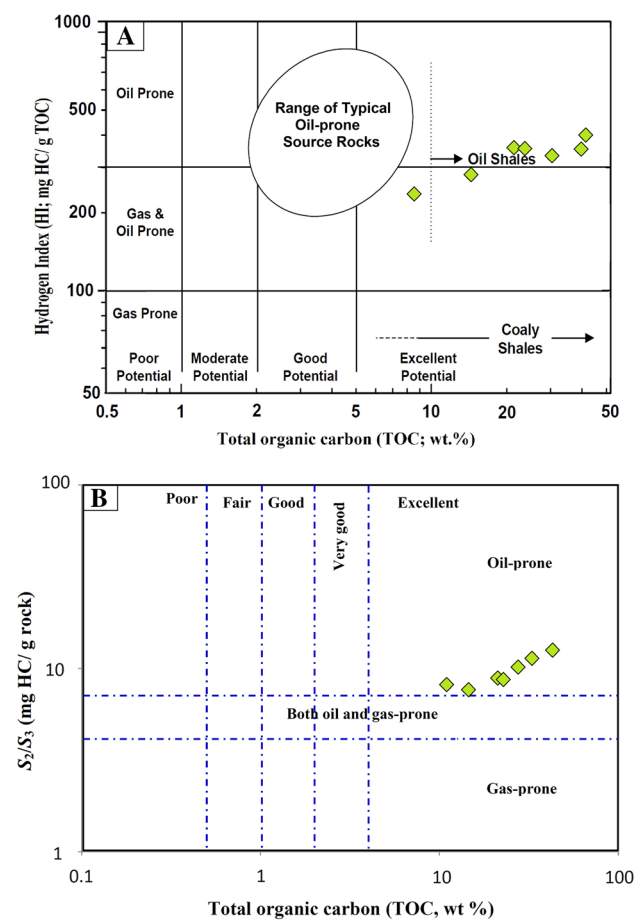

Fig. 12 Geochemical correlations between TOC content and Rock–Eval data (i.e., HI and S_2/S_3) parameters], implying that the analyzed bituminite shale samples are both oil- and gas-prone source rocks, with highly oil generation potential

the samples, the normal alkanes and isoprenoids display bimodal distribution of low to high molecular weight compounds, ranging from n-C_8 to n-C_{36} (Fig. 6). The carbon preference index (CPI) values were calculated using the distributions of normal alkane by the following equation: $CPI = [2(C_{23} + C_{25} + C_{27} + C_{29})/(C_{22} + 2(C_{24} + C_{26} + C_{28}] + C_{30})]$; and range from 1.98 to 2.30 (Table 1).

In addition to n-alkanes, the chromatograms of most of the samples are also the presence of the pristane (Pr) and phytane (Ph) isoprenoid hydrocarbons (Fig. 6). For most of the samples, the predominance of Pr over Ph (Fig. 6) results in a Pr/Ph ratio of more than 1 (1.17–2.70) as shown in Table 1. Additionally, isoprenoid ratios relative to n-alkane concentrations (C_{17}-C_{18}) were also determined as Pr/n-C_{17} and Ph/n-C_{18} ratios and found to be in the range of 0.20–0.69 and 0.20–0.31, respectively (Table 1).

Discussion

Organic matter input and environmental conditions

The organic matter input, its origin and the depositional environment of the analyzed bituminite shales were primarily investigated by applying normal alkane and isoprenoid in the saturated hydrocarbon together with microscopic results as previously described.

Normal alkanes and isoprenoids can permit postulating logical interpretations related to the nature of organic matter and its environmental conditions during deposition (Waples and Machihara 1991; Hadad et al. 2021).
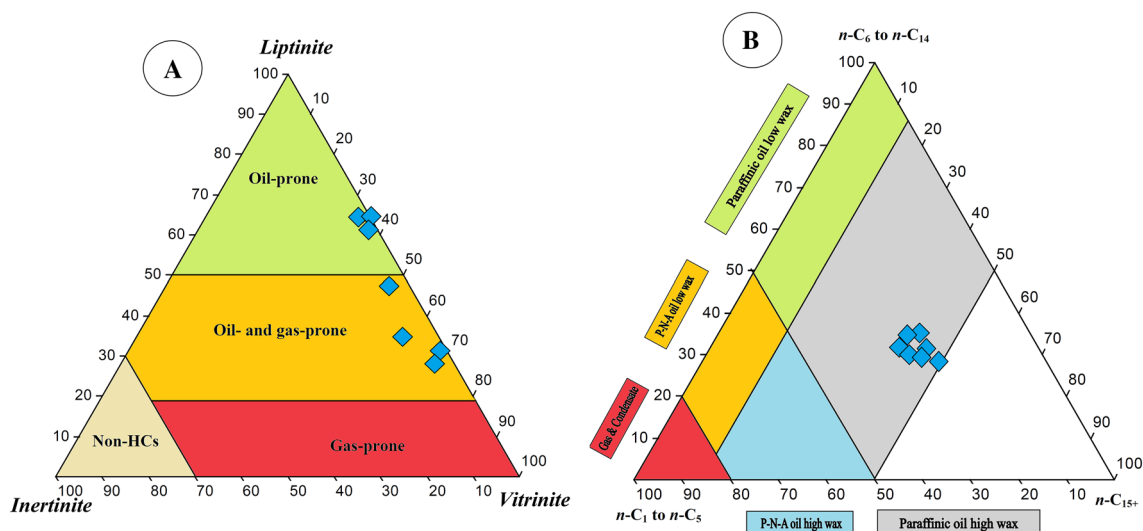
Fig. 13 Ternary diagrams on the petroleum types based on (**A**) the relative percentage of maceral types, and (**B**) relative percentages of pyrolyzate compounds, i.e., total resolved C_1 to C_5 hydrocarbons, the sum C_6 to C_{14}, and C_{+15} of the n-alkenes/n-alkane ranges, showing that the analyzed bituminite shale samples can generate mainly paraffinic oil with high wax content

In the present study, the normal alkanes and isoprenoids in the saturated HC fraction are portrayed by a bimodal distribution of low-medium molecular weight (n-C_8–n-C_{25}) and notable amounts of waxy alkanes ($+n$-C_{25}) as shown in Fig. 6. As a result, this distribution of n-alkanes suggests a mixture of organic matter of aquatic and terrestrial organic matter input (Alias et al. 2012; Sarki Yandoka et al. 2015).

The higher contributions from the aquatic organic matter and terrestrial source inputs into these shale sediments are compatible with isoprenoids and their Pr/Ph, Pr/n-C_{17} and Ph/n-C_{18} ratios. Such isoprenoid ratios can also aid interpretation of the paleodepositional environment as an indicator of redox conditions (e.g., Didyk et al. 1978; Ten Haven et al. 1987; Chandra et al. 1994; Peters et al. 2005; Tserolas et al. 2019). Generally, a low Pr/Ph ratio of less than 1.0 indicates strongly anoxic conditions commonly associated with a stratified water column, whereas a high Pr/Ph ratio of more than 3.0 is related to more terrestrial organic matter input under oxic environmental conditions (Didyk et al. 1978). In this regard, the studied bituminite shale samples with Pr/Ph values between 1.17 and 2.70 suggest suboxic environmental conditions during deposition. The isoprenoid Pr/n-C_{17} and Ph/n-C_{18} ratios further indicate high contributions of mixed organic matter inputs that were most likely deposited in suboxic to relatively anoxic environmental conditions (Fig. 7A). The combination between the isoprenoid ratios of Pr/Ph and Pr/n-C_{17} can also be used to provide information on organic matter input (e.g., Hughes et al. 1995; Williams et al. 1995; Hakimi et al. 2012; Alias et al. 2012; Sarki Yandoka et al. 2015). Marine organic matter usually has Pr/Ph ratios of less than 1 (Hakimi et al. 2012; Gharib et al. 2021; Hadad et al. 2021), while terrestrial organic matter has ratios of greater

than 3.0 (Alias et al. 2012; Sarki Yandoka et al. 2015). The relationship between Pr/Ph and Pr/n-C_{17} ratios suggests a mainly lacustrine organicmatter input (Fig. 8B). This interpretation of the organic matter input and the depositional environment of the analyzed bituminite shales are compatible with the geochemical proxies and maceral types that were observed under light microscopy.

The high TOC of up to 45.11 wt.% confirms the presence of the relatively reducing (suboxic-relatively anoxic) conditions that consequently enhanced the enrichment of organic matter during the deposition of the bituminite shale. However, the high TOC content is also correlated with low sulfur content and further shows that these bituminite shales being deposited in a non-marine environment (i.e., lacustrine), as shown in Fig. 8. The presence of the *Botryococcus* algae in some of the studied samples (Fig. 4d) is evident that the shales were deposited in freshwater lacustrine environments (e.g., Makeen et al. 2015).

Organic matter characterization and implications on source rock effectiveness and petroleum generation potential

This section discusses the potential of petroleum generation based on the characteristics of organic matter in the analyzed bituminite shales using integration multi-geochemical results and microscopic features of the organic facies.

The main factors controlling the amount of and type of petroleum generation in the source rocks are the organic richness and composition of the organic matter input (Dow 1977; Peters and Cassa 1994; Ardakani et al. 2017; Abdullah

Fig. 14 Geochemical cross-plots of (**A**) pyrolysis T_{max} vs. measured reflectance of huminite/vitrinite reflectance (VR$_o$ %) and (**B**) pyrolysis T_{max} vs. production index (PI), showing that the analyzed bituminite shale samples from Kapurdi mine are still at an immature stage for oil generation window
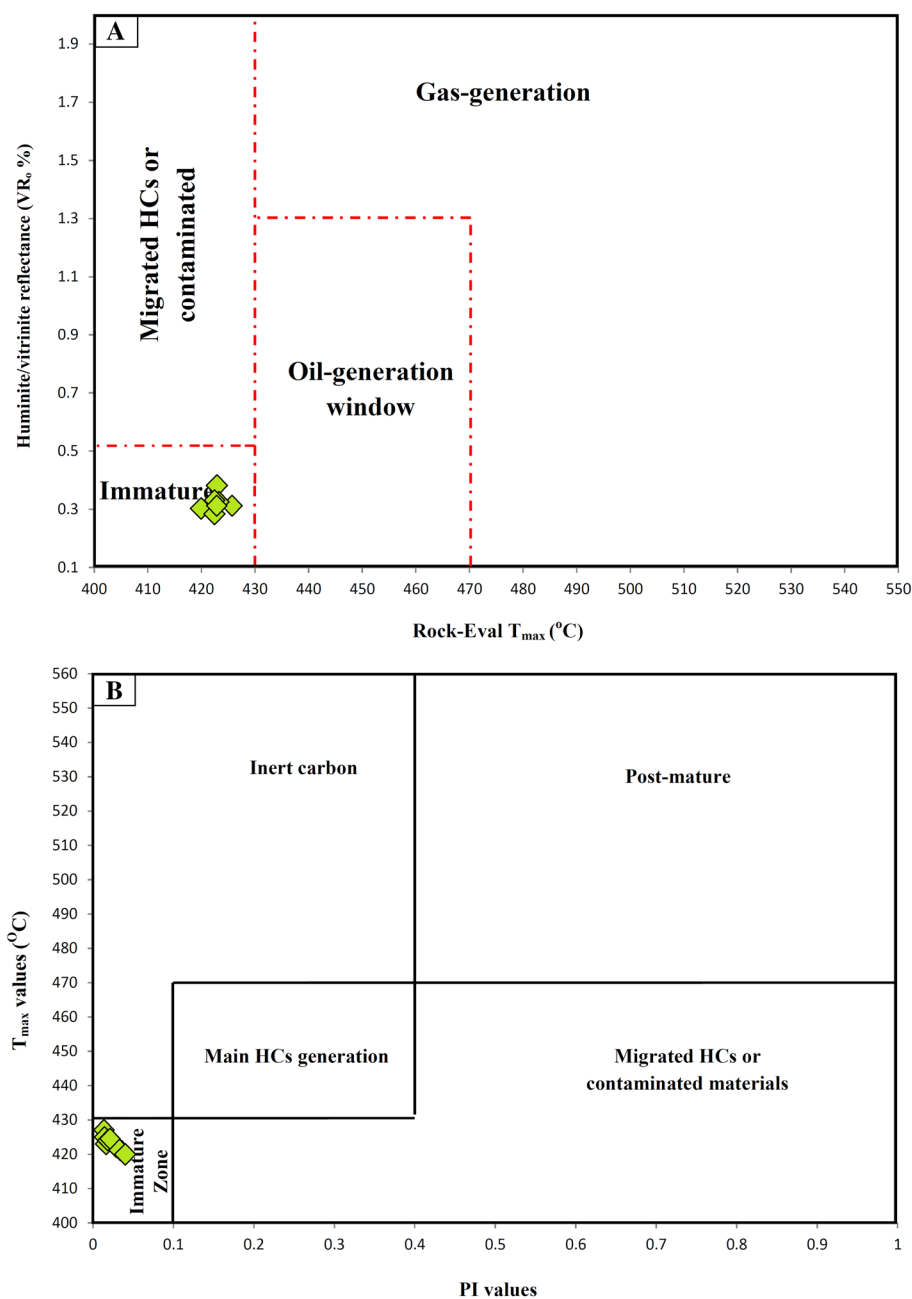
et al. 2017; Makeen et al. 2019; Aziz et al. 2020; Ahmad et al. 2022; Sohail et al. 2022).

The presence of adequate volumes of organic matter in the source rocks is the critical factor for controlling their generative potential once thermal maturity is attained (Peters 1986; Bordenave 1993; Peters and Cassa 1994; Aziz et al. 2020).This study presents high TOC contents from the investigated bituminite shale, overall, highlighting organic matter richness capable of generating hydrocarbons. The highest TOC content is correlated with high S_1 and S_2 yields and indicates that most of the analyzed bituminite shale samples have very good to excellent petroleum generative potential (Fig. 9).

The quality of organic matter in terms of kerogen typing is another critical factor in predicting the petroleum generation potential from source rocks (e.g., Espitalie et al. 1985; Peters and Cassa 1994; Mukhopadhyay et al. 1995; Aziz et al. 2020).

The presented Rock–Eval pyrolysis (i.e., the HI and OI) results show that most of the examined samples contain mainly Type II kerogen, with small contributions of mixed II/III kerogen as indicated from the van Krevelen diagram of HI against OI (Fig. 10a). The modified van Krevelen

diagram of programmed pyrolysis HI and T_{max} values also confirms the predominance of Type II kerogen, with mixed Type II/III kerogen and all fall within the immature zone (Fig. 10b).

In addition, the H/C and O/C atomic ratio is used to corroborate the kerogen characteristics (Hunt 1996; Erik 2011). The high ratios of H/C atomic indicate rich oil-prone Type I and II kerogens, while high O/C atomic indicates gas-prone Type III kerogen (Peters and Cassa 1994; Hunt 1996). Accordingly, the kerogen type in the analyzed bituminite shale samples is mainly oil-prone kerogen and classified as Types I and II based on their high ratio of H/C atomic in the range of 1.21–1.59 and low O/C atomic between 0.42 and 0.76 (Table 1). In this regard, four samples have Type II kerogen, while other three samples have Type I, as implied from the Van Krevelen's diagram of H/C and O/C atomic ratios (Fig. 10c).

The dominant presence of high n-alkene and n-alkane doublets with low amounts of light aromatic hydrocarbon (Fig. 5) suggests that the studied bituminite shales are likely to be oil-prone kerogen (e.g., Hasiah 1999; Harry 2008; Hakimi et al. 2013, 2015; Makeen et al. 2019). This interpretation of kerogen type is strongly demonstrated by a ternary plot modified by Eglinton et al. (1990), which used relative percentages of three pyrolyzate compounds, i.e., 2,3-dimethylthiophene, ortho-xylene, and carbon 9 (Fig. 11A).

This is further confirmed by the maceral types under microscope. However, when the results of the maceral composition in the analyzed samples (Table 1) were plotted on the Cornford (1979) ternary diagram, it was observed that the dominating organic matter is largely Type II kerogen, with small amounts of mixed Type II/III kerogen, as shown in Fig. 11B. The Type II kerogen is mainly consistent with hydrogen-rich liptinitic terrestrial organic matter, including alginite, sporinite, cutinite, resinite and bituminite (Fig. 4). Other samples with more than 60% and less than 80% of huminite macerals were likely to be Type II/III kerogen (Fig. 11B).

By evaluating the maceral composition and organic geochemical data, it is evident that these distributions of mainly Type II and II/III kerogen in the bituminite shale rocks are both oil- and gas-prone resources, with strong oil generation potential, as implied from the cross-plots of the TOC, HI, and S_2/S_3 geochemical data (Fig. 12A, B). The high contribution of oil generation potential from these bituminite shale rocks is confirmed by the high proportion of liptinitic materials (Fig. 13A). However, most of the hydrogen-rich liptinite macerals (i.e., sporinite, resinite, cutinite and suberinite) can generate paraffinic oil with a high waxy characteristic as reported by previously published works of Taylor et al. (1998) and Petersen et al. (2013) (Fig. 6). The high waxy characteristic of the expected oil to be generated from the analyzed samples is also consistent with the distributions

of n-alkene and n-alkane doublets in the Py–GC results (Fig. 5). The relative percentages of pyrolyzate compounds, i.e., total resolved C_1 to C_5 hydrocarbons, the sum C_6 to C_{14}, and C_{+15} of the n-alkenes/n-alkane ranges (Table 1) were plotted on the ternary diagram of Horsfield (1989) and indicate that the expected oil generating potential from the studied bituminite shale samples is mainly paraffinic oil, with high wax content (Fig. 13B).

Besides, the oil generation capacity of the analyzed bituminite shale samples was further assessed from the thermal maturation of the organic matter. The thermal maturity level of the analyzed bituminite shale samples was primarily evaluated using huminite/vitrinite reflectance (VR$_o$ %) data. These measurements are the best indicators in providing valuable information about the organic maturation and evolution of the petroleum generation capacity (Sweeney and Burnham 1990; Teichmüller et al. 1998). In this regard, the reflectance of the huminite/vitrinite in the studied samples was measured and found to be in low range between 0.29 and 0.35% (Table 1). This indicates that these bituminite shale rocks are still in immature stage and have not yet generated oil. The temperature of the maximum pyrolysis rate (T_{max}) is also commonly used to estimate the maturity of kerogens; as they mature, their T_{max} values increased (Bordenave 1993; Peters 1986; Tissot et al. 1987; Tissot and Welte 1984). However, the T_{max} is affected by several parameters, including migrated HCs, oil-based mud, and low pyrolysis response (Espitalie et al. 1985; Ahmed et al. 2022). The T_{max} values depend on the S_2 measurements, and the best T_{max} values were observed in samples with $S_2 > 1$ mg/g rock (Jarvie et al. 2001; Katz and Lin 2021). The analyzed samples of this study have S_2 of more than 70 mg/g rock (Table 1); hence, the maturation of the organic matter could be estimated through the measured T_{max} values. The T_{max} values of the samples range from 420 to 423 °C (Table 1), which indicates immature sources. This confirms the previously obtained VRo that agrees that most of the analyzed shales fall within the immature stage of the oil generation window (Fig. 14A).

The state of thermal maturity is further supported by the PI values obtained via the Rock–Eval pyrolysis. Low PI value of < 0.10 indicates immature organic matter, whereas a PI value between 0.10 and 0.40 suggests mature source rock (Peters 1986; Hazra et al., 2019). In agreement with the previously obtained VR$_o$ and T_{max} maturity data, the calculated PI values of less than 0.10 (Table 1) confirm that most of the studied shale samples are thermally immature source rocks (Fig. 14B). As a result, the organic matter of the bituminite shales collected from the Kapurdi mine has not yet reached the sufficient maturity levels to generate oil but can be recommended for oil shale retorting processes to release commercial amounts of oil upon using artificial heating techniques such as hydrothermal conversion.

Conclusions

The bituminite shale rocks from the Kapurdi mine in the northern Barmer Basin, NW India, were subjected to extensive organic geochemical and petrological analyses to investigate the characteristics of organic matter and the potential for oil generation. The conclusions from the results of this study are highlighted below.

- The analyzed bituminite shales have high TOC content of up to 45.11 wt.% and petroleum potential of up to 190.28 mg hydrocarbon/g rock, making them excellent source rocks for petroleum generation.
- The high TOC contents were correlated with low total sulfur content of < 1 wt. % and suggest a non-marine environment (i.e., lacustrine) during the deposition of these bituminite shale sediments. The dominant liptinitic terrestrial macerals with the presence of the *Botryococcus* algae confirm lacustrine environmental setting.
- The major portion of the analyzed bituminite shales is plotted along the hydrogen-rich kerogen (i.e. Types I, II and II/III), with high hydrogen index values (240 and 425 mg HC/g TOC) and high H/C atomic ratio of more than 1.20 as well as the dominant aliphatic *n*-alkene and *n*-alkane doublets with relatively minimal light aromatic components. This indicates that they are mainly oil-prone source rocks, with waxy paraffinic oil potential.
- The maturity-related indicators such as VR_o (< 40%) and T_{max} of < 430 °C show that the studied bituminite shale samples in the Kapurdi mine are still in an immature stage for oil generation. As a result, the attainment of the low thermal maturation level is not critical for converting the hydrogen-rich kerogen to the oil needed for commercial production.
- This study has shown that the bituminite shales in the Kapurdi mine are prospective unconventional petroleum resources. It can therefore be recommended for oil shale retorting processes to produce commercial amounts of oil using artificial heating techniques such as hydrothermal conversion.

Declarations

References

Abbassi S, Edwards DS, George SC, Volk H, Mahlstedt N, di Primio R, Horsfield B (2016) Petroleum potential and kinetic models for hydrocarbon generation from the Upper Cretaceous to Paleogene Latrobe group coals and shales in the Gippsland Basin, Australia. Org Geochem 91:54–67

Abdullah WH, Togunwa OS, Makeen YM, Hakimi MH, Mustapha KA, Baharuddin MH, Sia SG, Tongkul F (2017) Hydrocarbon source potential of Eocene-Miocene sequence of western Sabah, Malaysia. Mar Pet Geol 83:345–361

Aggarwal RK, Sharma A, Hussain S (2011) Geology and mineral resources of Rajasthan. Geol Surv India Misc Publ 30:1–130

Alias FL, Abdullah WH, Hakimi MH, Azhar MH, Kugler RL (2012) Organic geochemical characteristics and depositional environment of the tertiary Tanjong Formation coals in the Pinangah area, onshore Sabah, Malaysia. Int J Coal Geol 104:9–21

Ahmed A, Khan T, Jahandad S, Hakimi MH, Gharib AF, Kahal AY, Khan MA, Munir MN (2022) Organic matter characteristics of the Datta Shale formation and their contribution to conventional oil generation resources in the Upper Indus Basin, Northern Pakistan. Asian J Earth Sci. https://doi.org/10.1016/j.jseaes.2021.104975

Ambwani AK, Singh RS (1996) *Clavadiporopollenites raneriensis* gen. et sp. nov. from the tertiary sediments of Bikaner District, Rajasthan, India. Palaeobotanist 43:139–142

Ardakani OH, Sanei H, Ghanizadeh A, McMechan M, Ferri F, Clarkson CR (2017) Hydrocarbon potential and reservoir characteristics of lower Cretaceous Garbutt Formation, Liard Basin Canada. Fuel 209:274–289

ASTM D3176–09 (2009) Standard practice for ultimate analysis of coal and coke. Available at www.astm.org

Aziz H, Ehsan M, Ali A, Khan HK, Khan A (2020) Hydrocarbon source Rock–Evaluation and quantification of organic richness from correlation of well logs and geochemical data: a case study from the sembar formation, Southern Indus Basin, Pakistan. J Nat Gas Sci Eng 81:103433

Berner RA, Raiswell R (1983) Burial of organic carbon and pyrite sulfur in sediments over Phanerozoic time: a new theory. Geochem Cosmochim Acta 47:855–862

Bhowmick PK (2008) Phanerozoic petroliferous basin of India. Glimpses of Geoscience Research in India, pp 253–268

Bissada KK (1982) Geochemical constraints on petroleum generation and migration—a review. Proc ASCOPE Conf 81:69–87

Bordenave ML (1993) Applied petroleum geochemistry. Éditions Technip, Paris

Chandra K, Mishra CS, Samanta U, Gupta A, Mehrotra KL (1994) Correlation of different maturity parameters in the Ahmedabad-Mehsana block of the Cambay basin. Org Geochem 21:313–321

Cornford C (1979) Organic deposition at a continental rise; organic geochemical interpretations and synthesis at DSDP Site 397, eastern North Atlantic. Initial Rep Deep Sea Drill Proj 47:503–510

Dembicki Jr, H (1993) Improved determination of source quality and kerogen type by combining Rock–Eval and pyrolysis-gas chromatography results (abs.) AAPG Annual Convention Program, vol. 2, p 90

Dembicki H Jr (2009) Three common source Rock–Evaluation errors made by geologists during prospect or play appraisals. Am Assoc Pet Geol Bull 93:341–356

Dembicki H Jr, Horsfield HB, Ho TTY (1983) Source Rock–Evaluation by pyrolysis gas chromatography. Am Assoc Pet Geol Bull 67:1094–1103

Didyk BM, Simoneit BRT, Brassell SC, Eglinton G (1978) Organic geochemical indicators of palaeoenvironmental conditions of sedimentation. Nature 272:216–222

Dolson J, Burley SD, Sunder VR, Kothari V, Naidu B, Whiteley NP, Farrimond P, Taylor A, Direen N, Ananthakrishnan B (2015) The discovery of the Barmer Basin, Rajasthan, India, and its petroleum geology. AAPGBull 99(3):433–65

Dow WG (1977) Kerogen studies and geological interpretations. J Geochem Explor 7:79–99

Eglinton TI, Sinninghe Damsté JS, Kohnen MEL, de Leeuw JW (1990) Rapid estimation of the organic sulfur content of kerogens, coals and asphaltenes by pyrolysis-gas chromatography. Fuel 69:1394–1404

Erik NY (2011) Hydrocarbon generation potential and Miocene-Pliocene palaeoenvironments of the Kangal Basin (Central Anatolia, Turkey). J Asian Earth Sci 42:1146–1162

Espitalié J, Laporte JL, Madec M, Marquis F, Leplat P, Paulet J, Boutefeu A (1977) Methode rapid de characterisation des rocks meres, deleur potential petrolier et leurdegre devolution. Rev Inst Fr Pétrole 32:23–42

Espitalie J, Deroo G, Marquis F (1985) La pyrolyse Rock-Eval et ses applications. Rev Inst Fr Petrole 40:563–579

Farrimond P, Naidu BS, Burley SD, Dolson J, Whiteley N, Kothari V (2015) Geochemical characterization of oilsand their source rocks in the Barmer Basin, Rajasthan, India. Pet Geosci 21:301–321

Gharib AF, Özkan AM, Hakimi MH, Zainal Abidin N, Lashin A (2021) Integrated geochemical characterization and geological modeling of organic matter-rich limestones and oils from Ajeel Oilfield in Mesopotamian Basin. North Iraq Mar Pet Geol 126:104930

Hadad YT, Hakimi MH, Abdullah AH, Kinawy M, El Mahdy O, Lashin A (2021) Organic geochemical characteristics of Zeit source rock from Red Sea Basin and their contribution to organic matter enrichment and hydrocarbon generation potential. J Afr Earth Sci 177:104151

Hakimi MH, Abdullah WH, Shalaby MR (2012) Molecular composition and organic petrographic characterization of Madbi source rocks from the Kharir Oilfield of the Masila Basin (Yemen): palaeoenvironmental and maturity interpretation. Arab J Geosci 5:817–831

Hakimi MH, Abdullah WH, Sia SG, Makeen YM (2013) Organic geochemical and petrographic characteristics of tertiary coals in the northwest Sarawak, Malaysia: Implications for palaeoenvironmental conditions and hydrocarbon generation potential. Mar Pet Geol 48:31–46

Hakimi MH, Abdullah WH, Mustapha KA, Adegoke AK (2015) Petroleum generation modeling of the Late Cretaceous coals from the Jiza-Qamar basin as infer by kerogen pyrolysis and bulk kinetics. Fuel 154:24–34

Hakimi MH, Abdullah WH, Alqudah M, Makeen YM, Mustapha KA (2016) Organic geochemical and petrographic characteristics of the oil shales in the Lajjun area, Central Jordan: origin of organic matter input and preservation conditions. Fuel 181:34–45

Harry DJ (2008) Three common source Rock–Evaluation errors made by geologists during prospect or play appraisals. Am Assoc Pet Geol Bull 93:4341–4356

Hasiah AW (1999) Oil-generating potential of tertiary coals and other organic-rich sediments of the Nyalau Formation, onshore Sarawak. J Asian Earth Sci 17:255–267

Hazra B, Wood DA, Mani D, Singh PK, Singh AK (2019) Summary. In: Hazra B, Wood DA, Mani D, Singh PK, Singh AK (eds) Evaluation of shale source rocks and reservoirs. Springer, Cham, pp 139–142

Horsfield B (1989) Practical criteria for classifying kerogens: some observations from pyrolysis-gas chromatography. Geochim Cosmochim Acta 53:891–901

Hower JC, Wagner NJ (2012) Notes on the methods of the combined maceral/micro-lithotype determination in coal. Int J Coal Geol 95:47–53

Hughes WB, Holba AG, Dzou LIP (1995) The ratios of dibenzothiophene to phenanthrene and pristane to phytane as indicators of depositional environment and lithology of petroleum source rocks. Geochim Cosmochim Acta 59:3581–3598

Hunt JM (1996) Petroleum geochemistry and geology, 2nd edn. Freeman, New York, p 743

ICCP (2001) The new inertinite classification (ICCP system 1994). Fuel 80(4):459–471. https://doi.org/10.1016/s0016-2361(00)00102-2

Jarvie DM (1991) Total organic carbon (TOC) analysis. In: Merrill RK (ed) Treatise of petroleum geology: handbook of petroleum geology, source and migration processes and evaluation techniques. American Association of Petroleum Geologists, pp 113–118

Jarvie DM, Claxton BL, Henk F, Breyer JT (2001) Oil and shale gas from the Barnett Shale, Fort Worth basin, Texas. AAPG National Convention, June 3–6, 2001, Denver, CO, AAPG Bull. 85, 13 (Supplement), p A100

Kar RK, Sharma P (2001) Palynostratigraphy of late palaeocene and early eocene sediments of Rajasthan, India. Palaeontogr Abt Part B 256:123–157

Katz B, Lin F (2014) Lacustrine basin unconventional resource plays: key differences. Mar Pet Geol 56:255–265

Katz B, Lin F (2021) Consideration of limitations of thermal maturity with respect to vitrnite reflectance, Tmax and other proxies. Am Assoc Pet Geol Bull 105:695–720

Lafargue E, Marquis F, Pillot D (1998) Rock-Eval 6 applications in hydrocarbon exploration, production, and soil contamination studies. Rev Institut Fr Pet. https://doi.org/10.2516/ogst:1998036

Larter SR (1984) Application of analytical pyrolysis techniques to kerogen characterization and fossil fuel exploration/exploitation. In: Voorhees K (ed) Analytical pyrolysis. Heinemann, Butterworths, London, pp 212–275

Makeen YM, Abdullah WH, Hakimi MH, Mustapha KA (2015) Source rock characteristics of the Lower Cretaceous Abu Gabra Formation in the Muglad Basin, Sudan, and its relevance to oil generation studies. Mar Petrol Geol 59:505–516

Makeen YM, Abdullah WH, Abdul Ghofur MN, Ayinla HA, Hakimi MH, Shan X, Mustapha KA, Kamal Shuib M, Liang Y, Zainal Abidin NS (2019) Hydrocarbon generation potential of oligocene

oil shale deposit at onshore Penyu basin, Chenor, Pahang, Malaysia. Energy Fuels 33:89–105

Mathews RP, Singh BD, Singh VP, Singh A, Singh H, Shivanna M, Dutta S, Mendhe VA, Chetia R (2020) Organo-petrographic and geochemical characteristics of Gurha lignite deposits, Rajasthan, India: insights into the palaeovegetation, palaeoenvironment and hydrocarbon source rock potential. Geosci Front 11:965–988

Mukherjee AK, Alam MM, Mazumdar SK, Haque R, Gowrisankaran S (1992) Physico-chemical properties and petrographic characteristics of the Kapurdi lignite deposit, Barmer basin, Rajasthan, India. Int J Coal Geol 21:31–44

Mukhopadhyay PK, Wade JA, Kruge MA (1995) Organic facies and maturation of Jurassic/Cretaceous rocks, and possible oil-source rock correlation based on pyrolysis of asphaltenes, Scotion Basin, Canada. Org Geochem 22:85–104

Paul S, Dutta S (2016) Terpenoid composition of fossil resins from western India: New insights into the occurrenceof resin-producing trees in Early Paleogene equatorial rainforest of Asia. Int J Coal Geol 167:65–74

Peters KE (1986) Guidelines for evaluating petroleum source rock using programmed pyrolysis. Am Assoc Pet Geol Bull 70:318–329

Peters K, Cassa M (1994) Applied source rock geochemistry. The petroleum system from source to trap. Am Assoc Pet Geol Mem 60:93–117

Peters KE, Walters CC, Moldowan JM (2005) The biomarker guide 2: biomarkers and isotopes in petroleum exploration and Earth history, 2nd edn. Cambridge University Press, Cambridge, p 704

Petersen HI, Øverland JA, Solbakk T, Bojesen-Koefoed JA, Bjerager M (2013) Unusual resinite-rich coals found in northeastern Greenland and along the Norwegian coast: Petrographic and geochemical composition. Int J Coal Geol 109–110:58–76

Pickel W, Kus J, Flores D, Kalaitzidis S, Christanis K, Cardott BJ, Misz-Kennan M, Rodrigues S, Hentschel A, Hamor-Vido M, Crosdale P, Wagner N (2017) Classification of liptinite—ICCP system 1994. Int J Coal Geol 169:40–61

Rana RS, Kumar K, Singh H, Rose KD (2005) Lower vertebrates from the Late Palaeocene–earliest Eocene Akli Formation, giral lignite mine, Barmer District, Western India. Current Science, pp 1606–1613

Raju SV, Mathur N (2013) Rajasthan lignite as a source of unconventional oil. Curr Sci 104:752–757

Sarki Yandoka BM, Abdullah WH, Abubakar MB, Hakimi MH, Adegoke AK (2015) Geochemical characterisation of early Cretaceous lacustrine sediments of Bima formation, Yola Sub-basin, Northern Benue Trough, NE Nigeria: Organic matter input, preservation, paleoenvironment and palaeoclimatic conditions. Mar Pet Geol 61:82–94

Shivanna M, Singh H (2016) Depositional environment and hydrocarbon potential of marginal marine sediments of Eocene from western India: a palynofacies perspective. Mar Petrol Geol 73:311–321

Shivanna M, Singh A, Singh BD, Singh VP, Matthews RP, Souza PA (2017) Peat biomass degradation: evidence from fungal and faunal

activity in carbonized wood from the Eocene sediments of western India. Palaeoworld 26:531–542

Shukla A, Mehrotra RC, Spicer RA, Spicer TEV, Kumar M (2014) Cool equatorial terrestrial temperatures and the South Asian monsoon in the early Eocene: evidence from the Gurha mine, Rajasthan, India. Palaeogeo Palaeoclim Palaeoecol 412:187–198

Singh AK, Kumar A (2018) Petrographic and geochemical study of Gurha lignites, Bikaner basin, Rajasthan, India: Implications for thermal maturity, hydrocarbon generation potential and paleodepositional environment. J Geol Soc India 92:27–35

Singh AK, Hakimi MH, Kumar A, Ahmed A, Abidin NSZ, Kinawy M, Mahdy OE, Lashin A (2020) Geochemical and organic petrographic characteristics of high bituminous shales from Gurha mine in Rajasthan, NW India. Sci Rep 10:22108. https://doi.org/10.1038/s41598-020-78906-x

Sohail GM, Radwan AE, Mahmoud M (2022) A review of Pakistani shales for shale gas exploration and comparison to North American shale plays. Energy Rep 8:6423–6442

Sýkorová I, Pickel W, Christanis K, Wolf M, Taylor GH, Flores D (2005) Classification of huminite—ICCP system 1994. Int J Coal Geol 62:85–106

Sweeney JJ, Burnham AK (1990) Evaluation of a simple model of vitrinite reflectance based on chemical kinetics. Am Assoc Pet Geol Bull 74:1559–1570

Taylor GH, Teichmüller M, Davis ACFK, Diessel CFK, Littke R, Robert P (1998) Organic petrology. Gebrüder Borntraeger, Berlin, pp 86–174

Teichmüller M, Littke R, Robert P (1998) Coalification and maturation. In: Teichmüller M, Davis A, Diessel CF, Littke R, Robert P, Taylor GH (eds) Organic petrology. Gebrüder Borntraeger, Berlin, pp 86–174

Ten Haven HL, de Leeuw JW, Rullkötter J, Damsté JSS (1987) Restricted utility of the pristane/phytane ratio as a palaeoenvironmental indicator. Nature 330:641–643

Tissot BP, Welte DH (1984) Petroleum formation and occurrence, 2nd edn. Springer, Berlin, p 699

Tissot BP, Pelet R, Ungerer PH (1987) Thermal history of sedimentary basins, maturation indices, and kinetics of oil and gas generation. Am Assoc Pet Geol Bull 71:1445–1466

Tserolas P, Maravelis AG, Tsochandaris N, Pasadakis N, Zelilidis A (2019) Organic geochemistry of the Upper Miocene-Lower Pliocene sedimentary rocks in the Hellenic Fold and Thrust Belt, NW Corfu Island, Ionian sea, NW Greece. Mar Pet Geol 106:17–29

Waples DW, Machihara T (1991) Biomarkers for geologists: A practical guide to the application of steranes and triterpanes in petroleum geology. AAPG Methods in Exploration, 2, 5–10

Williams A, Kloster A, Duckworth R, Piggott N (1995) The role of the Airborne Laser Fluorosensor (ALF) and other seepage detection methods in exploring frontier basins. In: Hansjien S (ed) Petroleum exploration and exploitation in Norway. NPF Special Publication, pp 421–431